Rapid Ambiguity Resolution using Multipath Spatial Processing for High Accuracy Carrier Phase

Alison Brown, Kees Stolk, *NAVSYS Corporation*

BIOGRAPHY

Alison Brown is the President and CEO of NAVSYS Corporation. She has a PhD in Mechanics, Aerospace, and Nuclear Engineering from UCLA, an MS in Aeronautics and Astronautics from MIT, and an MA in Engineering from Cambridge University. In 1986, she founded NAVSYS Corporation. Currently she is a member of the Interagency GPS Executive Board Independent Advisory Team and Scientific Advisory Board for the USAF and serves on the GPS World editorial advisory board.

Kees Stolk is a GPS/INS Engineer at NAVSYS Corporation working with simulation, design, and testing of real-time GPS/Inertial systems, array signal processing multipath estimation and reduction, spatial signal processing, sensor integration by Kalman filtering. He has an MSc in Electrical Engineering from Twente University of Technology, Netherlands.

ABSTRACT

The largest error component on the carrier-phase observations is generally caused by carrier-phase multipath offsets. This generally results in a slow oscillating cyclic offset which must be averaged (either through satellite or vehicle motion) before reliable ambiguity resolution can be performed for kinematic positioning. NAVSYS has developed a digital spatial processing receiver that uses the spatial degrees of freedom within an antenna array to minimize multipath errors on the carrier-phase observations. This in turn makes the ambiguity solution more reliable and reduces the number of processing cycles needed to result in a kinematic position fix. In this paper, test results are presented showing the reduction in the carrier phase errors when using this approach. Kinematic positioning test results are also shown using the HAGR digital beam-steering GPS receiver.

INTRODUCTION

Multipath errors are caused by the receiver tracking a composite of the direct GPS signals and reflected GPS signals from nearby objects, such as the ground, a building or ship's mast (see Figure 1). Multipath errors can be observed by their effect on the measured signal/noise ratio and the code and carrier observations, as described below.[1,2,3]

Signal/Noise Ratio When multipath is present, the signal/noise ratio magnitude varies due to the constructive and destructive interference effect. The peak-to-peak variation is an indication of the presence of multipath signals, as shown by the following equation where A is the amplitude of the direct signal, A_M is the amplitude of the reflected multipath signal, θ is the carrier phase offset for the direct signal and θ_M is the carrier phase offset for the multipath signal.

$$\widetilde{A} = \left| A + A_M e^{\Delta\theta} \right| - A$$

$$\widetilde{\theta} = \angle(A + A_M e^{\Delta\theta})$$

$$\Delta\theta = \theta - \theta_M$$

The multipath carrier phase error ($\widetilde{\theta}$) is related to the received multipath power level from the above equation. This results in a cyclic carrier phase error as the multipath signals change from constructive to destructive interference that has the peak-to-peak carrier phase error shown in Figure 3. Multipath also causes the signal-to-noise ratio to vary between the peak and minimum levels shown in Figure 2 depending on the relative Multipath/Signal (M/S) strength. For low elevation GPS satellite signals, it is quite common to get M/S received power levels as high as -3 dB. This will cause a cyclic error on the carrier phase observations of around +/- 2 cm.

For precision Kinematic Carrier Phase Tracking (KCPT) GPS applications, this error will affect the ability to perform rapid carrier cycle ambiguity resolution. Analysis performed for KCPT applications, such as the Shipboard Relative GPS (SRGPS) Joint Precision Approach and Landing System (JPALS), has determined that M/S levels must be below –12 dB to meet the program's objectives for reliable carrier phase ambiguity resolution. Testing performed by NAVAIR on the USS Theodore Roosevelt has indicated that conventional GPS antenna solutions, such as those shown in Figure 4, do not meet this objective. In this paper, preliminary test results are included that show the performance advantages of a digital beam-steering receiver for minimizing multipath effects and providing precision kinematic GPS positioning.
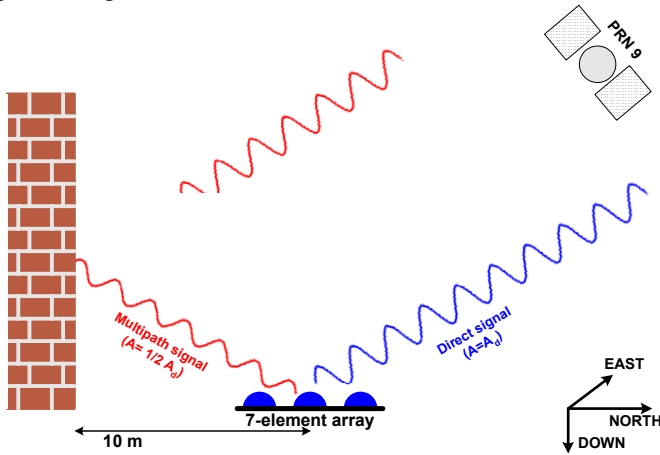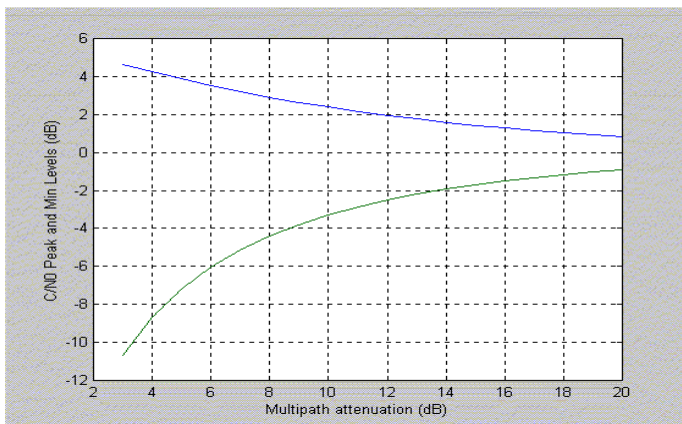

Figure 3 Multipath Peak Phase error vs. Attenuation (dB)

Figure 1 Typical Multipath Scenario

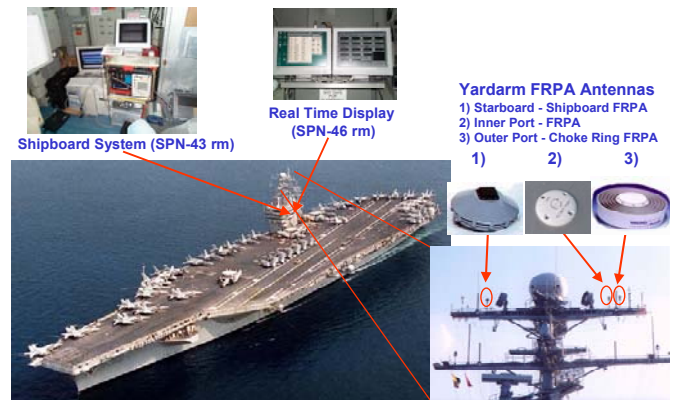**Figure 2 Multipath Amplitude Effect**

Figure 4 Shipboard Relative GPS Carrier Landing Test Installation

HAGR PRINCIPLE OF OPERATION

The NAVSYS High-gain Advanced GPS Receiver (HAGR) is a digital beam steering receiver designed for GPS satellite radio navigation and other spread spectrum applications. This is available for both military and commercial precision GPS applications and uses the modular assembly shown in Figure 5 to allow it to be easily configured to meet a user's specific requirements.

The HAGR system architecture is shown in Figure 6. The signal from each antenna element is first digitized using a Digital Front-End (DFE). This bank of digital signals is then used to create the composite digital beam-steered signal input for each of the receiver channels by applying a complex weight to combine the antenna array outputs. As shown in Figure 6, the array weights are applied independently for each of the satellite channels. This allows the antenna array pattern to be optimized for each satellite signal tracked.

The weights for each channel are dynamically downloaded through software control. The HAGR software can automatically calculate the beam steering

pattern for each satellite based on the known receiver location, the broadcast GPS satellite location and the input attitude of the antenna array. For static applications, the array can either be configured pointing north (the default attitude) or the actual attitude is programmed into the configuration file. For mobile applications, the antenna array attitude is input through a serial port from either a magnetic compass and tilt sensor or and inertial navigation system. The HAGR also includes a mode where the antenna weights are read from a user definable file based on the satellite azimuth and elevation. Matlab tools exist for creating these antenna weights based on specific user requirements.

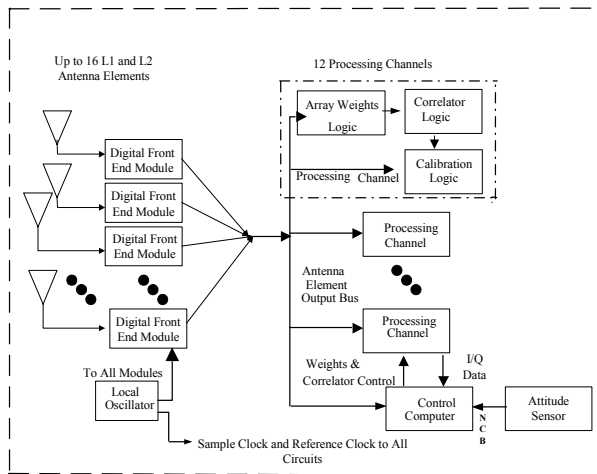**Figure 5 HAGR Assembly**

Figure 6 HAGR System Architecture

In Figure 7 and Figure 8, the antenna patterns created by the digital antenna array are shown for four of the satellites tracked. The HAGR can track up to 12 satellites simultaneously. The antenna pattern provides the peak in the direction of the satellite tracked (marked 'x' in each figure). The beams follow the satellites as they move across the sky. Since the L2 wavelength is larger than the L1 wavelength, the antenna beam width is wider for the L2 antenna pattern than for the L1.
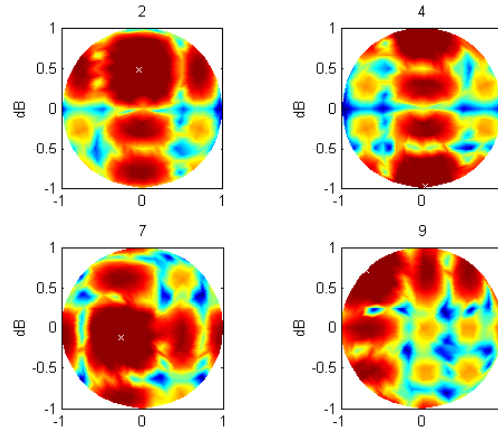

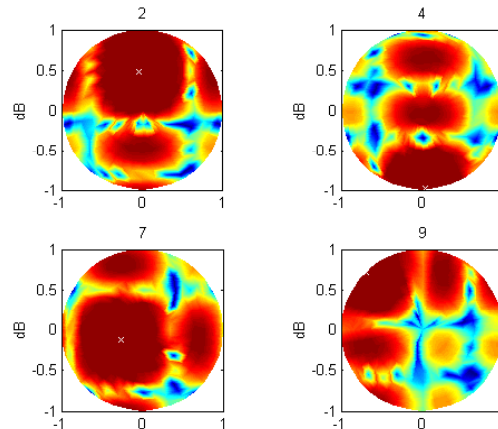**Figure 7 L1 Antenna Pattern**

Figure 8 L2 Antenna Pattern

KINEMATIC POSITIONING ALGORITHM

The steps followed by the relative kinematic positioning algorithm developed by NAVSYS are illustrated in Figure 9. Kinematic positioning and alignment relies on the relationship of the carrier phase observations to the range observations described in the following equation.

Equation 1

$$PR_1 = R + bu_1 + bsv_{PR1} + T + I_1 + n_{PR1}$$

$$PR_2 = R + bu_2 + bsv_{PR2} + T + I_1 \frac{\lambda_2^2}{\lambda_1^2} + n_{PR2}$$

$$-CPH_1 = R + bu_{CPH1} + bsv_{CPH1} + T - I_1 + n_{CPH1} - N_1 \lambda_1$$

$$-CPH_2 = R + bu_{CPH2} + bsv_{CPH2} + T - I_1 \frac{\lambda_2^2}{\lambda_1^2} + n_{CPH2} - N_2 \lambda_2$$

where
PR = pseudo-range on L1 or L2 frequencies (meters)
CPH = carrier phase on L1 or L2 frequencies (meters)
R_T = true range (meters)
bu = range equivalent receiver clock offset (meters)
bsv = range equivalent satellite clock offset (meters)
T = tropospheric delay (meters)
I = ionospheric delay (meters)
n = measurement noise (meters)
N = CPH integer (cycles)
λ = carrier wavelength (meters)

The pseudo-range observations observe the range from the GPS satellites to the UE (R) offset by the user and satellite clock (b), the tropospheric delay (T) and the ionospheric delay (I). The ionospheric delay is different on the L1 and L2 observations as it is inversely proportional to the frequency squared and so can be removed from the PR by differencing. The DGPS corrections will remove any errors in the navigation solution caused by satellite position and clock offsets. The accuracy of the PR derived DGPS corrected position solution is a function of the pseudo-range noise which includes receiver noise and multipath errors. The GPS/inertial navigation solution will filter the short term noise effects, but it cannot correct for correlated noise errors from multipath. This results in the final DGPS corrected solution accuracy are generally on the order of 1 to 1.5 meters due to these uncorrected errors.

The effect of multipath is much smaller on the GPS carrier phase observations. As shown in Equation 1, the carrier phase (CPH) observation provides the same observability of user position through the range to the GPS satellite but includes an additional uncertainty of the integer number of cycles to the satellite (N). If this integer ambiguity is resolved, then the position accuracy derived from the CPH observation accuracy is a function of the carrier phase noise and carrier multipath errors which are on the order of a few centimeters. The process of resolving this integer cycle ambiguity is generally termed cycle ambiguity resolution and is the key to performing kinematic GPS positioning.

The steps employed by the kinematic positioning algorithm to resolve the integer ambiguity are illustrated in Figure 9 and described below.
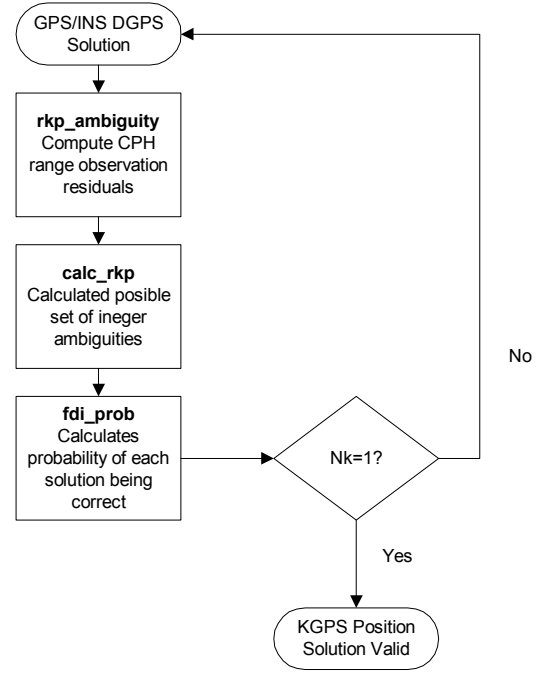
Figure 9 Kinematic Positioning Algorithm

rkp_ambiguity
The first step is to create the carrier phase corrected measurement residuals. These are derived from the following equation and include: carrier phase corrections (CPC) from the reference location, estimated range to the satellite from the DGPS solution and the estimated atmospheric errors (tropo and iono). As shown in the following equation, this measurement residual observes the position error in the DGPS solution (relative to the reference location), the residual ionospheric and tropospheric errors and the integer ambiguity offset. This reduces the ambiguity resolution process to a single (wide-lane) ambiguity $N_W = N_1 - N_2$. The wide-lane wavelength is 86 cm as opposed to the L1 wavelength of 19 cm. This larger resolution wavelength is easier to observe allowing ambiguity resolution to occur much faster with L1/L2 dual frequency observations than for single frequency (L1 only) GPS. To remove the effect of the clock bias, the single-differenced observations are used (zsd) since the clock bias is common between the GPS satellite observations

Equation 2

$$z_{CPH1} = -CPH_1 - \hat{R} - \hat{b}_{svCPH1} + C\hat{P}C_1 - \Delta\hat{T} + \Delta\hat{I}_1$$

$$= \underline{1}^T \tilde{\underline{x}} + bu_{CPH1} + (\tilde{T} - \tilde{I}_1) + n_{CPH1} - N_1 \lambda_1$$

$$z_{CPH2} = -CPH_2 - \hat{R} - \hat{b}_{svCPH2} + C\hat{P}C_2 - \Delta\hat{T} + \Delta\hat{I}_2$$

$$= \underline{1}^T \tilde{\underline{x}} + bu_{CPH1} + (\tilde{T} - \tilde{I}_1 \frac{\lambda_2^2}{\lambda_1^2}) + n_{CPH2} - N_2 \lambda_2$$

$$z_{CPHW} = \left(\frac{z_{CPH1}}{\lambda_1} - \frac{z_{CPH2}}{\lambda_2} \right) \lambda_W$$

$$= \underline{1}^T \, \underline{\tilde{x}} + bu_{CPH1} + \underline{\tilde{T}} - \tilde{I}_1 \frac{\lambda_W}{\lambda_1} \left(1 - \frac{\lambda_2}{\lambda_1} \right)$$

$$+ n_{CPH1} \frac{\lambda_W}{\lambda_1} - n_{CPH2} \frac{\lambda_W}{\lambda_2} - N_W \lambda_W$$

$$\lambda_W^{-1} = \lambda_1^{-1} - \lambda_2^{-1} \qquad N_W = N_1 - N_2$$

calc_rkp

The purpose of the calc_rkp function is to compute the set of possible ambiguities for each of the satellite observations. This is performed by computing all of the likely ambiguities based on an initial search space that the ambiguity solution must fall within (see Figure 10). The search space is dictated by the initial uncertainty of the GPS/inertial navigation solution (P_{DGPS}). Each ambiguity must pass the following criteria to be considered a valid member of the ambiguity set (Nset). The geometry vector H is calculated from the satellite line of sight vectors. The scale factor α is computed based on the desired probability of missed detection for the KGPS solution, based on the equation below.

Equation 3

$$\underline{N}\underline{N}^T < \alpha \, H \, E\left[\underline{\tilde{x}} \underline{\tilde{x}}^T \right] H^T / \lambda_W^2 = \alpha \, H \, \frac{P_{DGPS}}{\lambda_W^2} H^T \qquad \underline{N} \in Nset$$
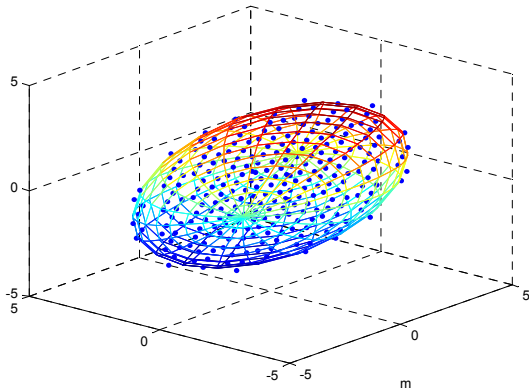
$$P_{MD} = \chi^2(\alpha|3)$$

Figure 10 GPS/Inertial Solution Space Ambiguity Set

fdi_prob

The correct ambiguity from the set is isolated by using an integrity check to reject the incorrect solutions. For the correct ambiguity solution, the fault vector (f), computed from the following equation will include only the receiver noise errors. For all other values, the f vector will also include errors due to the ambiguity error.

Equation 4

$$\underline{f} = S(N_W \lambda_W + \underline{z}_{CPHW})$$

$$= S\left(H\underline{\tilde{x}} + \underline{\tilde{T}} - \tilde{I}_1 \frac{\lambda_W}{\lambda_1} \left(1 - \frac{\lambda_2}{\lambda_1} \right) + \underline{n}_{CPH1} \frac{\lambda_W}{\lambda_1} - \underline{n}_{CPH2} \frac{\lambda_W}{\lambda_2} \right) \approx \underline{n}$$

$$S = I - HH^* \qquad SH = 0 \qquad H^* = \left(H^T H \right)^{-1} H^T$$

The S matrix has Nsv-4 degrees of freedom. As the number of GPS satellites in the solution increases, the ability to distinguish between the different members of Nset improves, and also the initial DGPS search space ellipse gets smaller. The f vector is accumulated over multiple samples to determine the correct ambiguity. The smaller the noise (n) on the observation, the faster the algorithm can differentiate between the different ambiguities and pick the correct solution to allow kinematic positioning to be performed.

Pseudo-Range and Carrier-Phase GPS Corrections

The pseudo-range and carrier-phase correction messages are generated using observations from a reference receiver. The pseudo-range corrections are used to compute the DGPS navigation solution. The carrier-phase corrections are used to compute the KGPS positioning solution. The messages generated include the following information. This format is in accordance with RTCM SC-104 [4].

PRC Message (repeated for each of Nsvs on L1 and L2)

- Time — GPS time of correction
- PRN — SVID correction applies to
- PRC — Pseudo-range correction (meters)
- RRC — Rate of change of correction (m/s)
- IOD — Issue of data for related ephemeris used
- Sigma_prc — Estimated accuracy of correction (m)

CPC Message (repeated for each of Nsvs on L1 and L2)

- Time — GPS time of correction
- PRN — SVID correction applies to
- CPC — Carrier-phase correction (meters)
- DCPC — Rate of change of correction (m/s)
- CLOC — Loss of phase lock counter (indicates ambiguity must be recomputed)
- Sigma_cph — Estimated accuracy of correction (m)

MULTIPATH TESTING

At the time of writing this paper, only a single digital beam-steering L1/L2 HAGR was available for testing. To evaluate the multipath performance improvements, testing

was performed by partitioning the HAGR 7-element antenna array (see Figure 11) into two 4-element sub-arrays as shown in Figure 12. The carrier phase errors provided by the individual antenna elements and the digital beam-steered results from the two sub-arrays was compared. When a full 7-element HAGR array is used, further performance improvements could be expected over the dual 4-element test results presented here. To quantify the level of multipath, both the carrier phase relative to the center element and the signal amplitude is plotted in Figure 13 and Figure 14. From the peak-to-peak variation of the IQ amplitude, $A_{pp} \approx 40$, and phase, $\Delta\theta \approx 2cm$, we can see that the signal to multipath ratio is roughly 5 dB using a single element (see Figure 2 and Figure 3).

Figure 13 Amplitudes of array 1 elements (5s moving average)
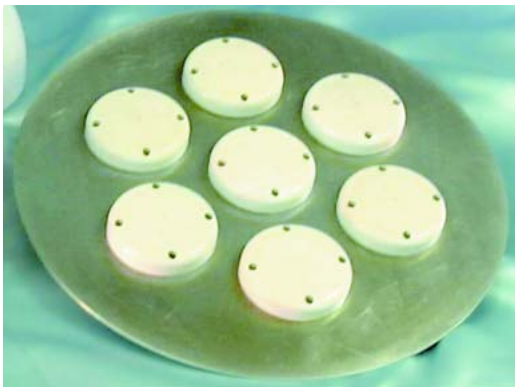
Figure 11 HAGR 7-Element Array
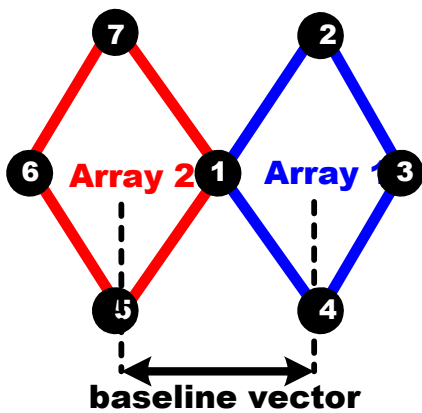
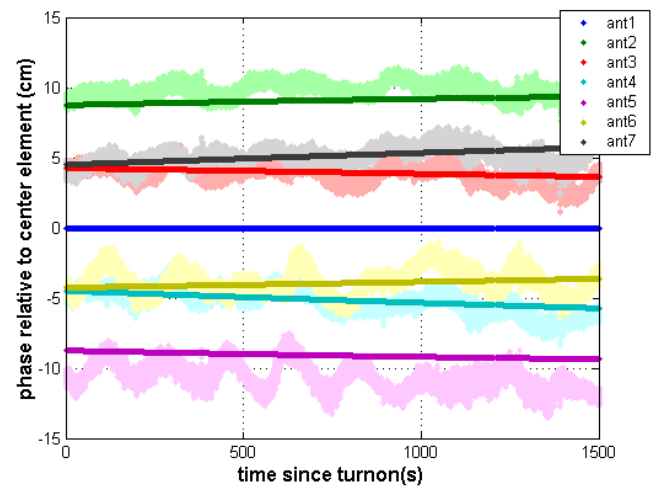**Figure 12 HAGR Dual Sub-array Test Setup**

Figure 14 Carrier Phase of array 1 (thick lines: expected phase offset)

The spatial information from the 7-element phased array was also processed to identify the source of the multipath through direction of arrival (DOA) estimation using the MUSIC algorithm. The results shown in Figure 15 shows both the direct signals and a strong multipath signal being receiver from the NAVSYS' building
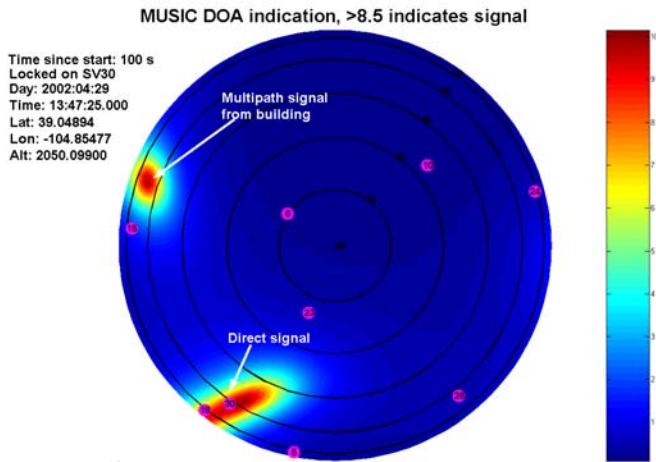
Figure 15 MUSIC direction of arrival estimation

To test the single element and the digital beam-steered carrier phase accuracy, the carrier phase errors were compared between the center element and the two 4-element sub-arrays. These results are plotted in Figure 16 for both the single element and the beam-steered results. From this figure, the peak-to-peak phase error is in the order of 3.5 cm when using a single antenna element. With digital beamforming the phase error is reduced to about 1 cm. The amplitude of the multipath is derived from the peak phase variation seen in Figure 16 and referencing Figure 3.

$$\Delta\theta_{pp} \approx 1cm \longrightarrow SMR = 10dB$$

This test shows that the required signal to multipath ratio of 10 dB is realized when using only a 4-element sub-array. A 7-element array will provide further improvements allowing the signal to multipath ratio goal of 12 dB to be achieved.
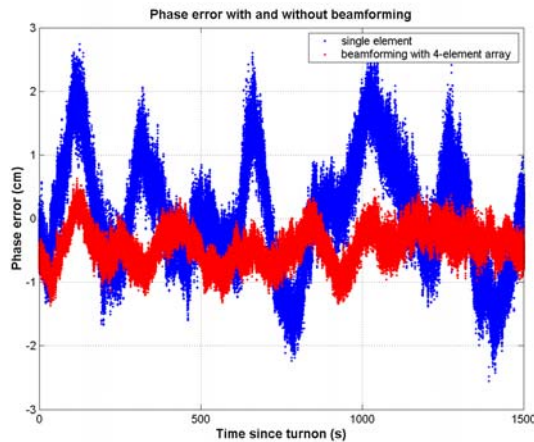

**Figure 16 Single Element and Digital Beam-Steered Carrier Phase Errors**

HAGR KINEMATIC POSITIONING TEST DATA

To demonstrate the precise positioning performance possible when using the HAGR for kinematic positioning, a test was performed using the HAGR receiver located at NAVSYS facilities and the Alternate Master Clock (AMC2) reference station operating at Schriever AFB some 25 miles distant. The results from this kinematic positioning solution are shown in Figure 17 and Figure 18. The RMS position variation is between 2 to 9 cm on each axis (see Figure 18). .
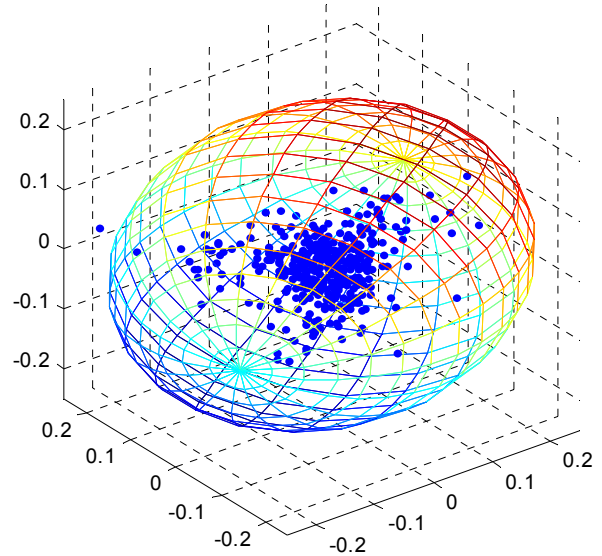

Figure 17 HAGR Widelane Kinematic Position (relative to AMC2)
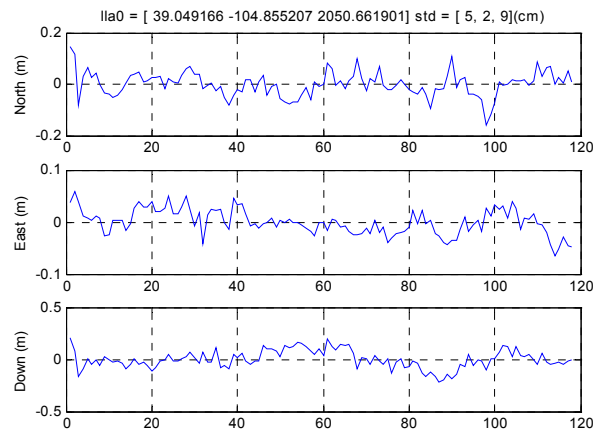
Figure 18 NED Widelane Position Variation (m)

The KGPS algorithm also estimates the carrier phase noise from the fault vector. From Figure 19 this converges to a value of within 1 cm (0.04 cycles) for the L1 and L2 phase measurements. This phase noise includes both the effect of the HAGR carrier phase errors

and also the AMC2 carrier phase errors. Further testing is planned at a later date to evaluate the performance improvements that could be achieved using a HAGR receiver as both the reference station and the remote unit for kinematic positioning
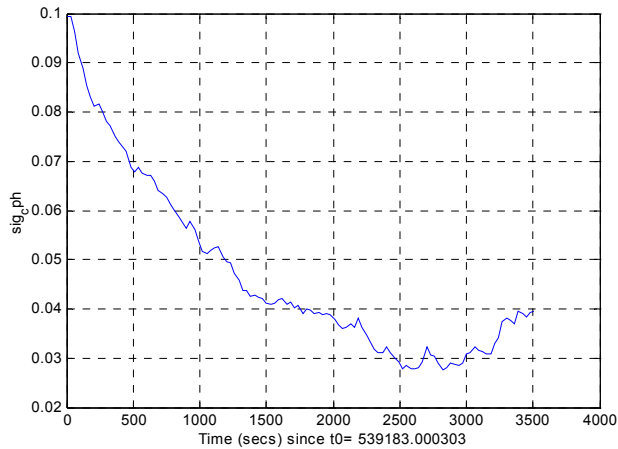
Figure 19 Estimated Carrier Phase Noise from Fault Vector (cycles)

CONCLUSION

The testing performed to date has shown that there is a significant reduction in the peak-to-peak carrier phase error from multipath when using a digital beamsteering receiver. With dual 4-element sub-arrays, the peak-to-peak carrier phase error attributed to multipath was less than 1 cm compared to 3.5 cm when using a single antenna element. With a larger antenna array, the performance could be expected to further improve. The HAGR kinematic GPS position solution when operating with the AMC2 reference station located at Schriever AFB was within 2 – 9 cm (RMS) on each axis. This performance includes the carrier phase errors from both the HAGR and the AMC2 reference station. Further testing is planned at a later date to show what further performance improvements could be achieved when using a HAGR as both a reference station and a remote receiver.

ACKNOWLEDGEMENT

REFERENCES

1 A. Brown, ""Performance and Jamming Test Results of a Digital Beamforming GPS Receiver," Proceedings of Joint Conference on Navigation, Orlando, Florida, May, 2002.

2 A. Brown, N. Gerein, "Test Results from Digital P(Y) Code Beamsteering Receiver for Multipath Minimization," ION 57th Annual Meeting, Albuquerque, New Mexico, September 2001.

3 A. Brown, "High Accuracy GPS Performance using a Digital Adaptive Antenna Array," Proceedings of ION National Technical Meeting 2001, Long Beach, CA, January 2001

4 RTCM Recommended Standards for Differential GNSS (Global Navigation Satellite Systems Service), RTCM SC-104, Version 2., January 3, 1994